Mendeleev Communications

Mendeleev Commun., 2025, **35**, 307–309

Mechanisms of influence of divalent Mg cation on DNA–Dps complex revealed by molecular modeling methods

Ksenia B. Tereshkina,*[a] Vladislav V. Kovalenko,[a] Valentin A. Manuvera,[b] Eduard V. Tereshkin,[a] Victoriya V. Potokina,[c] Yurii F. Krupyanskii[a] and Nataliya G. Loiko*[c]

[a] *N. N. Semenov Federal Research Center for Chemical Physics, Russian Academy of Sciences, 119991 Moscow, Russian Federation. E-mail: ksenia.tereshkina@chph.ras.ru*
[b] *Lopukhin Federal Research & Clinical Center of Physical-Chemical Medicine of Federal Medical Biological Agency, 119435 Moscow, Russian Federation*
[c] *Federal Research Centre 'Fundamentals of Biotechnology' of the Russian Academy of Sciences, 119071 Moscow, Russian Federation. E-mail: loikonat@mail.ru*

DOI: 10.71267/mencom.7623

The destructive effect of divalent cations Mg^{2+} on the crystal structure of the DNA–Dps complex was explored. It was shown using the classical molecular dynamics methods that this effect resulted from a decrease of interaction between the N-termini of the Dps protein and DNA when the concentration of Mg^{2+} in the system increases, and important Mg^{2+} binding sites in the protein and DNA molecules were determined. It is concluded that the preferential interaction of DNA and protein oxygen atoms with the Mg^{2+} cation leads to the weakening of their mutual bonds and destruction of the DNA–Dps complex.

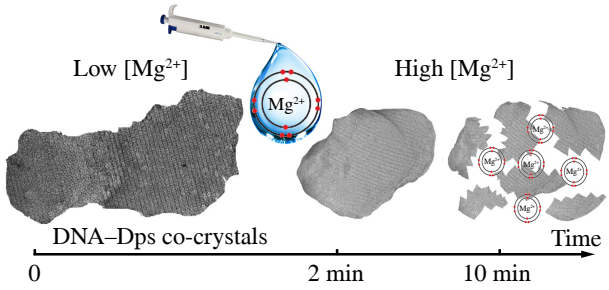

Keywords: DNA–Dps complex, DNA-binding protein Dps, divalent Mg cation, *Escherichia coli*, classical molecular dynamics.

Protection of DNA from various types of stress is one of the main tasks of any living organisms. Prokaryotes synthesize large numbers of copies of the DNA-binding protein Dps to preserve DNA during prolonged periods of starvation.[1,2] This protein, due to its unique properties, interacts with DNA to form a protective complex.[3,4] To date, more than a thousand Dps-like proteins have been identified in bacteria (~97%) and archaea (~3%).[5] All of them are characterized by a common three-dimensional architecture in the form of spherical dodecamers with a central cavity.[6] The dodecameric structure of the *Escherichia coli* Dps protein is very compact, but each of the 12 monomers has a flexible disordered protruding N-terminus consisting of 25 amino acid residues.[7] Studies of *E. coli* Dps have shown that three lysine residues at positions 5, 8, and 10 and an arginine residue at position 18 in these disordered N-termini of the protein are responsible for the formation of the complex with DNA.[7] The removal of the first 8 or 18 amino acids drastically reduces the ability of Dps to bind to DNA and aggregate with other Dps molecules.[8] Thus, the interaction of Dps with DNA is currently viewed as a strong electrostatic interaction between the positively charged N-terminal ends of the protein and the negatively charged DNA backbone.

The process of the DNA–Dps complex formation and its subsequent stability is influenced by a number of physical[9] and chemical factors,[10] including the concentration of divalent ions.[11,12] Previously we have shown that the addition of Mg^{2+} cations (in the form of an aqueous $MgCl_2$ solution) to pre-formed *in vitro* DNA–Dps co-crystals leads to the deformation of the crystal lattice, crushing of the crystal, and its gradual disintegration within 10 min.[11] It was suggested that this occurs as a result of the weakening of electrostatic interactions between DNA and the N-termini of Dps due to the effect of Mg^{2+} cations on DNA.

Since magnesium is an obligatory component of the bacterial cytoplasm, it appears that varying its intracellular content is a mechanism to control the strength of the DNA–Dps complex. A decrease in the concentration of divalent ions around the nucleoid leads to the formation of a stable DNA–Dps co-crystal and the transition of bacterial cells to a quiescent state[13]. An increase in the ion concentration, on the contrary, promotes the breakdown of the complex, the release of DNA, and the return of bacteria to active life. Elucidating the exact details of this biochemical and biological mechanism is not only of important scientific interest. The ability to manipulate the metabolic activity of bacterial cells holds great promise in biotechnology, medicine, and collection activities.

In this work, we continued to investigate the mechanism of the effect of the divalent cation Mg^{2+} on the stability of the DNA–Dps complex using modern molecular dynamics methods, which have proven themselves in the study of Dps protein properties.[9,14]

The *in silico* studies were preceded by *in vitro* experiments that further confirmed the detrimental effect of Mg^{2+} on the DNA–Dps co-crystal (see Online Supplementary Materials for details). At the first stage the large single crystals 1.54 ± 0.38 μm in size were obtained [Figure 1(*a*)]. The crystals had a high degree of ordering as indicated by clear multiple peaks in the Fourier image [Figure 1(*b*)]. Addition of Mg^{2+} cations to the solution with crystals (at a ratio of 1200 cations per 1 protein molecule) after 2 min of incubation reduced the size of the complexes to 0.42 ± 0.09 μm, maintaining their periodicity only along one direction (with a pitch of 7.5 nm) [Figures 1(*c*),(*d*)]. After 10 min, the complete dissolution of the crystals was

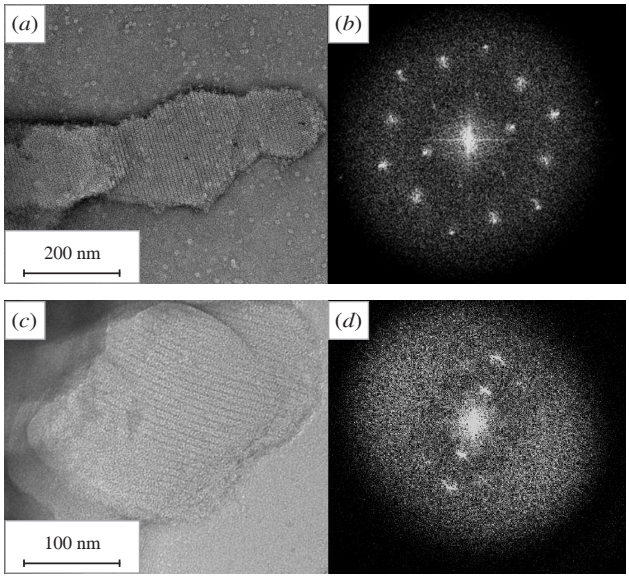

Figure 1 Transmission electron microscopy (TEM) images of (*a*),(*c*) DNA–Dps crystals and (*b*),(*d*) corresponding Fourier transforms; (*a*),(*b*) DNA–Dps crystals obtained on a carbon-coated copper TEM grid by mixing 3 μl of Dps (3.4 mg cm^{-3}), 1.5 μl of DNA (0.25 ng cm^{-3}), and 1.5 μl of EDTA (0.14 mmol dm^{-3}); (*c*),(*d*) semi-degraded DNA–Dps crystals 2 min after addition of 0.5 μl of 10 mM $MgCl_2$ solution.

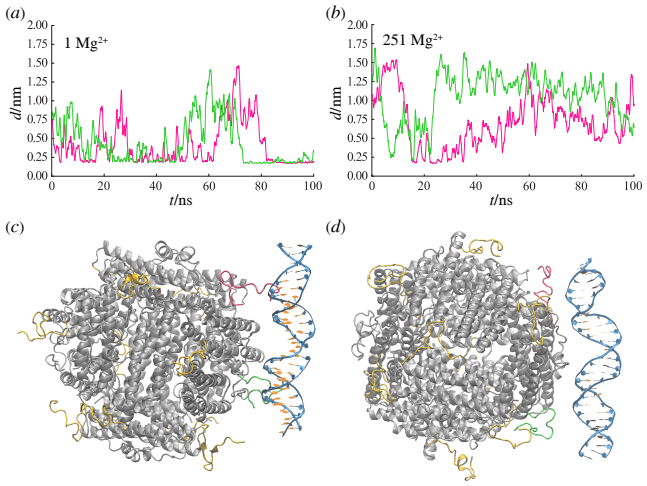

Figure 2 Minimum distances between the closest-to-DNA N-termini of the Dps protein (1–25 amino acid residues of every Dps subunit) at the concentration of Mg^{2+}: (*a*) 1 cation per periodic box and (*b*) 251 cations per periodic box. The structure of the DNA–Dps complex (at 100 ns) at the concentration of Mg^{2+}: (*c*) 1 cation per periodic box and (*d*) 251 cations per periodic box. Dps is red, DNA is blue, non-bonding N-termini are gold, and closest N-termini and corresponding curves are pink and green. The data are given for systems containing one DNA molecule (25 base pairs) and one Dps molecule. The temperature of simulation is 28 °C.

observed. Decreasing the concentration of Mg^{2+} cations added to DNA–Dps crystals increased the time of their destruction.

The molecular mechanisms of the processes occurring with the Dps protein[15] and DNA–Dps complex formation in the presence of Mg^{2+} cations were explored using molecular dynamics (MD) methods[16–19] (see Online Supplementary Materials for details).

The interaction of DNA and the Dps protein mediated by the N-terminal regions of the protein was monitored by the distance between the atoms of each of the N-termini and DNA. Atoms (not linked by a covalent bond) were considered to interact tightly if the distance between them was $d \leqslant 0.5$ nm.[15] Simulations showed that at a concentration of Mg^{2+} equal to 1 ion per periodic box (corresponding to the cytoplasmic concentration in *E. coli* cells), the DNA molecule contacts one or two N-termini throughout the entire observation period of 100 ns [Figures 2(*a*),(*c*)]. When the Mg^{2+} concentration is increased to 251 ions per periodic box (which corresponds to a concentration of ~130 mmol dm^{-3} at the surface of the macromolecules), these interactions practically cease, since the atoms of the N-termini and DNA diverge by a distance exceeding *d* and do not come closer until the end of the simulation [Figures 2(*b*),(*d*)].

The MD trajectory analysis showed that the distribution of Mg^{2+} cations in water in the systems containing Dps and DNA corresponds to the experimental data for aqueous solutions of $MgCl_2$.[20–22] Magnesium ions acquire a hydration shell, which first layer consists of six water molecules. The main binding sites of Mg^{2+} cations in the protein molecule[23] predictably are the negatively charged oxygen atoms of the side groups of Asp and Glu and the nitrogen atoms of His. To a lesser extent, they interact with oxygen atoms of the side groups of Asn and Gln. Figures S1(*a*)–(*c*) show examples of the replacement of two-to-five oxygen atoms in the hydration shell with oxygen or nitrogen atoms of the Dps protein. It is worth noting that in systems with a high concentration of Mg^{2+}, the cations interact not only with atoms of the side groups of the amino acid residues, but also with oxygen atoms of the protein backbone [Figure S1(*b*): Leu104, Figure S1(*c*): Pro108, Leu109, and Ile111]. At a high concentration of Mg^{2+}, the directly contacting Mg^{2+}, and Cl^- ions also appear, which is not typical for dilute aqueous solutions of $MgCl_2$ (where the ions are usually separated by hydration shells).[20–23] The latter two interact with nitrogen atoms of the side groups of Lys residues. Nitrogen atoms carry a positive charge and determine the DNA-binding ability of the lysine residues in the Dps protein, as mentioned above. Their shielding can affect the ability of the protein to bind to DNA. It is also shown that Mg^{2+} directly attack the root amino acids of the N-termini, the negatively charged region of the protein, and the amino acid residues adjacent to them. Figure S1(*d*) shows that the major magnesium binding sites in the protein are the amino acid residues Asp20, Glu25, Glu64, Asp75, Asp78, Glu82, Asp110, and Asp142 (and adjacent residues). But it is noteworthy that the average number of Mg^{2+} per amino acid residue along the trajectory is less than one. As for DNA [Figure S1(*e*)], on the contrary, any pair of bases at any moment of the trajectory contacts to one or more Mg^{2+} ions. No significant preference was observed for the binding of ions to one of the four DNA bases (adenine, guanine, thymine, or cytosine). However, it has been noted that the DNA bases closest to the protein are subject to a more intensive attack from magnesium ions. Probably, Mg^{2+} cations, entering the space between the protein and DNA, are retained in the DNA grooves, competing with side groups of N-terminal lysine residues.

The pairwise interactions of Mg^{2+} ions with the protein were also investigated based on the MD trajectories. All types of protein atoms with a negative partial charge not close to zero according to the force field were considered. The results were analyzed based on the radial distribution functions (RDFs), which allow one to make a detailed consideration of correlations in pairwise interactions. Correlations were analyzed in groups of atoms of the protein main chain, protein side chains, all types of amino acid residues, atoms in different positions within these residues, and Mg^{2+}. This made it possible to identify the main groups of atoms contacting with magnesium. It was found that oxygen atoms make the greatest contribution to the Mg^{2+}–protein interactions, nitrogen atoms to a lesser extent, and the contribution of other atoms is insignificant. This is consistent with the data obtained above (Figure S1). Figure 3 shows the most significant interactions of Mg^{2+} with a protein [Figures 3(*a*)–(*c*)] and DNA [Figure 3(*d*)]. In the radial distribution curves, the peaks at $r \approx 2$ Å indicate direct interactions of atoms, peaks at $r \approx 4$ Å indicate interactions through one hydration shell, *etc*. The overall interaction of Mg^{2+} with all oxygen atoms of the protein [Figure 3(*a*)] is

largely contributed by the atoms of the protein side chain, and to a lesser extent by the protein main chain. Nevertheless, the contribution of the latter is quite large. That is, Mg^{2+} binds to the main chain of the protein, which may affect its spatial characteristics. The main sites of magnesium binding to the oxygen atoms of the protein side groups are the amino acid residues Asp, Gln, Glu, and Asn (in the order of decreasing first and second peaks). As for the binding to nitrogen atoms [Figure 3(*c*)], the main role belongs to the His residues and some contribution from other side chain nitrogen atoms is observed, but their peak is shifted from 2 to 2.5 Å.

As for the interaction of Mg^{2+} ions with DNA [Figure 3(*d*)], the interactions with all three structural elements of DNA nucleotides were considered: nitrogenous bases, deoxyribose[24] residues, and phosphoric acid residues. The contribution to the interaction of Mg^{2+} with oxygen atoms[24] is made to a greater extent by the oxygen atoms of phosphoric acid residues. The interaction of magnesium ions apparently occurs also directly with the oxygen atoms of nitrogenous bases and deoxyribose. There is virtually no binding of magnesium to DNA *via* nitrogen atoms.

Thus, this work, carried out using classical molecular dynamics methods, has supplemented the available data on the mechanisms of DNA–Dps complex degradation in the presence of a large amount of Mg^{2+} cations. Once in the co-crystal region, the Mg^{2+} cations begin to interact with oxygen and nitrogen atoms of DNA and the protein, which leads to the breakage of bonds between DNA and N-terminal sites of Dps. The effect of Mg^{2+} on the protein is not limited to the N-termini of the protein, but occurs throughout the entire protein volume. At high concentrations of magnesium, DNA is the first to be attacked by Mg^{2+}, in the grooves of which the cations probably begin to compete with the lysine side groups, preventing the latter from binding to DNA.

The computations were performed using MVS-10P at the Joint Supercomputer Center of the Russian Academy of Sciences. Experimental data were obtained using the analytical transmission electron microscope JEM-2100 (JEOL, Japan) at the Unique equipment setup '3D-EMC' of Moscow State University. The research was financially supported by the Russian Science Foundation (grant no. 23-24-00250).

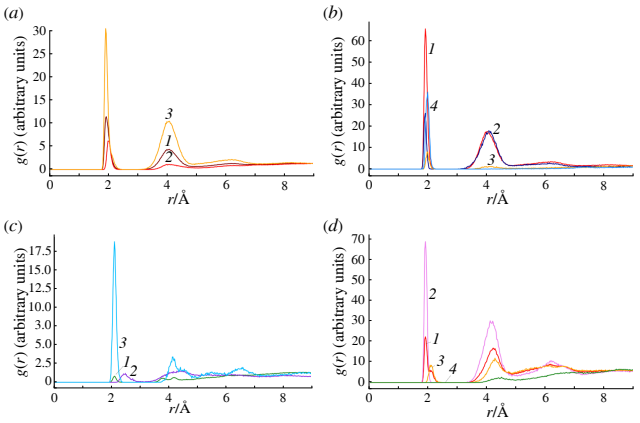

Figure 3 Radial distribution functions (RDFs) of Mg^{2+} with oxygen and nitrogen atoms of DNA and Dps: (*a*) RDF of Mg^{2+} ions and oxygen atoms of Dps. The following atoms of Dps were taken into account: (*1*) all oxygen atoms, (*2*) oxygen atoms only of the protein main chain, and (*3*) oxygen atoms only of the protein side chain. (*b*) RDF of Mg^{2+} ions and oxygen atoms of the side chains of (*1*) Asp, (*2*) Glu, (*3*) Asn, and (*4*) Gln. (*c*) RDF of Mg^{2+} ions and nitrogen atoms of Dps. The following atoms of Dps were taken into account: (*1*) all nitrogen atoms, (*2*) nitrogen atoms only of the protein side chain, and (*3*) nitrogen atoms of the His side chain. (*d*) RDF of Mg^{2+} ions and oxygen and nitrogen atoms of DNA: (*1*) all oxygen atoms, (*2*) oxygen atoms of phosphoric acid residues, (*3*) oxygen atoms of deoxyribose and nitrogenous bases, and (*4*) all nitrogen atoms.

Online Supplementary Materials

Supplementary data associated with this article can be found in the online version at doi: 10.71267/mencom.7623.

References

1 M. Almirón, A. J. Link, D. Furlong and R. Kolter, *Genes Dev.*, 1992, **6(12b)**, 2646; https://doi:10.1101/gad.6.12b.2646.
2 D. Frenkiel-Krispin and A. Minsky, *J. Struct. Biol.*, 2006, **156**, 311; https://doi.org/10.1016/j.jsb.2006.05.014.
3 N. Loiko, K. Tereshkina, V. Kovalenko, A. Moiseenko, E. Tereshkin, O. S. Sokolova and Y. Krupyanskii, *Biology*, 2023, **12**, 853; https://doi.org/10.3390/biology12060853.
4 K. Orban and S. E. Finkel, *J. Bacteriol.*, 2022, **204**, e00036-22; https://doi.org/10.1128/jb.00036-22.
5 T. Haikarainen and A. C. Papageorgiou, *Cell. Mol. Life Sci.*, 2010, **67**, 341; https://doi.org/10.1007/s00018-009-0168-2.
6 S. M. Williams and D. Chatterji, in *Macromolecular Protein Complexes III: Structure and Function. Subcellular Biochemistry*, eds. J. R. Harris and J. Marles-Wright, Springer, Cham, 2021, vol. 96, pp. 177–216; https://doi.org/10.1007/978-3-030-58971-4_3.
7 R. A. Grant, D. J. Filman, S. E. Finkel, R. Kolter and J. M. Hogle, *Nat. Struct. Biol.*, 1998, **5**, 294; https://doi.org/10.1038/nsb0498-294.
8 P. Ceci, S. Cellai, E. Falvo, C. Rivetti, G. L. Ross and E. Chiancone, *Nucleic Acids Res.*, 2004, **32**, 5935; https://doi.org/10.1093/nar/gkh915.
9 N. G. Loiko, E. V. Tereshkin, V. V. Kovalenko, Y. F. Krupyanskii and K. B. Tereshkina, *Microbiology*, 2023, **92**, S78; https://doi.org/10.1134/S0026261723603640.
10 V. V. Melekhov, U. S. Shvyreva, A. A. Timchenko, M. N. Tutukina, E. V. Preobrazhenskaya, D. V. Burkova, V. G. Artiukhov, O. N. Ozoline and S. S. Antipov, *PLoS One*, 2015, **10**, e0126504; https://doi.org/10.1371/journal.pone.0126504.
11 A. Moiseenko, N. Loiko, K. Tereshkina, Y. Danilova, V. Kovalenko, O. Chertkov, A. V. Feofanov, Y. F. Krupyanskii and O. S. Sokolova, *Biochem. Biophys. Res. Commun.*, 2019, **517**, 463; https://doi.org/10.1016/j.bbrc.2019.07.103.
12 L. Dadinova, R. Kamyshinsky, Y. Chesnokov, A. Mozhaev, V. Matveev, A. Gruzinov, A. Vasiliev and E. Shtykova, *Int. J. Mol. Sci.*, 2021, **22**, 6056; https://doi.org/10.3390/ijms22116056.
13 N. G. Loiko, N. E. Suzina, V. S. Soina, T. A. Smirnova, M. V. Zubasheva, R. R. Azizbekyan, D. O. Sinitsyn, K. B. Tereshkina, Yu. A. Nikolaev, Yu. F. Krupyanskii and G. I. El'-Registan, *Microbiology*, 2017, **86**, 714; https://doi.org/10.1134/S002626171706011X.
14 K. B. Tereshkina, E. V. Tereshkin, V. V. Kovalenko, Y. F. Krupyanskii and N. G. Loiko, *Mendeleev Commun.*, 2025, **35**, 148; https://doi.org/10.71267/mencom.7567.
15 V. Kovalenko, A. Popov, G. Santoni, N. Loiko, K. Tereshkina, E. Tereshkin and Y. Krupyanskii, *Acta Crystallogr., Sect. F: Struct. Biol. Commun.*, 2020, **F76**, 568; https://doi.org/10.1107/S2053230X20012571.
16 B. Hess, C. Kutzner, D. van der Spoel and E. Lindahl, *J. Chem. Theory Comput.*, 2008, **4**, 435; https://doi.org/10.1021/ct700301q.
17 E. V. Tereshkin, N. G. Loiko, K. B. Tereshkina, V. V. Kovalenko and Y. F. Krupyanskii, *Russ. J. Phys. Chem. B*, 2022, **16**, 726; https://doi.org/10.1134/S1990793122040285.
18 A. M. Toikka and A. V. Petrov, *Mendeleev Commun.*, 2023, **33**, 413; https://doi.org/10.1016/j.mencom.2023.04.036.
19 C. Zhang, C. Zhang, Y. Meng, T. Li, Z. Jin, S. Hou and C. Hu, *Mendeleev Commun.*, 2022, **32**, 334; https://doi.org/10.1016/j.mencom.2022.05.013.
20 R. Caminiti, G. Licheri, G. Piccaluga and G. Pinna, *J. Appl. Crystallogr.*, 1979, **12**, 34; https://doi.org/10.1107/s0021889879011729.
21 G. Pálinkás, T. Radnai, W. Dietz, Gy. I. Szász and K. Heinzinger, *Z. Naturforsch., A: Phys. Sci.*, 1982, **37**, 1049; https://doi.org/10.1515/zna-1982-0912.
22 E. Duboué-Dijon and D. Laage, *J. Phys. Chem. B*, 2015, **119**, 8406; https://doi.org/10.1021/acs.jpcb.5b02936.
23 E. A. Groisman, K. Hollands, M. A. Kriner, E.-J. Lee, S.-Y. Park and M. H. Pontes, *Annu. Rev. Genet.* 2013, **47**, 625; https://doi.org/10.1146/annurev-genet-051313-051025.
24 M. G. Khrenova, T. I. Mulashkina, R. A. Stepanyuk and A. V. Nemukhin, *Mendeleev Commun.*, 2024, **34**, 1; https://doi.org/10.1016/j.mencom.2024.01.001.

Received: 17th September 2024; Com. 24/7623